JOURNAL OF VIROLOGY, Nov. 1990, p. 5519–5528
0022-538X/90/115519-10$02.00/0

Vol. 64, No. 11

Unique Amino Acid Substitutions in the Capsid Proteins of Foot-and-Mouth Disease Virus from a Persistent Infection in Cell Culture

J. DÍEZ,[1] M. DÁVILA,[1] C. ESCARMÍS,[1] M. G. MATEU,[1] J. DOMINGUEZ,[1] J. J. PÉREZ,[2†] E. GIRALT,[2] J. A. MELERO,[3] AND E. DOMINGO[1*]

Centro de Biología Molecular, Universidad Autónoma de Madrid, Canto Blanco, 28049 Madrid,[1] Department de Química Orgànica, Universitat de Barcelona, 08028 Barcelona,[2] and Centro Nacional de Microbiología, Virología e Inmunología Sanitarias, Majadahonda, 28220 Madrid,[3] Spain

Received 22 May 1990/Accepted 3 August 1990

Maintenance of a persistent foot-and-mouth disease virus (FMDV) infection in BHK-21 cells involves a coevolution of cells and virus (J. C. de la Torre, E. Martínez-Salas, J. Díez, A. Villaverde, F. Gebauer, E. Rocha, M. Dávila, and E. Domingo, J. Virol. 62:2050–2058, 1988). The resident FMDV undergoes a number of phenotypic changes, including a gradual decrease in virion stability. Here we report the nucleotide sequence of the P1 genomic segment of the virus rescued after 100 passages of the carrier cells (R100). Only 5 of 15 mutations in P1 of R100 were silent. Nine amino acid substitutions were fixed on the viral capsid during persistence, and three of the variant amino acids are not represented in the corresponding position of any picornavirus sequenced to date. Cysteine at position 7 of VP3, that provides disulfide bridges at the FMDV fivefold axis, was substituted by valine, as determined by RNA, cDNA, and protein sequencing. The modified virus shows high buoyant density in cesium chloride and depicts the same sensitivity to photoinactivation by intercalating dyes as the parental FMDV C-S8c1. Amino acid substitutions fixed in VP1 resulted in altered antigenicity, as revealed by reactivity with monoclonal antibodies. In addition to defining at the molecular level the alterations the FMDV capsid underwent during persistence, the results show that positions which are highly invariant in an RNA genome may change when viral replication occurs in a modified environment.

Foot-and-mouth disease virus (FMDV) is an aphthovirus that causes an economically important disease of cattle and other cloven-hooved animals. Inapparent, persistent infections of the upper respiratory tracts of ruminants (53) represent a reservoir of virus (4, 24, 25, 49, 50) and a potential source of antigenic variants (22). We have established BHK-21 cell lines persistently infected with FMDV that provide a model system to explore mechanisms of long-term virus and cell survival. One such cell line, C_1-BHK-Rc1, was initiated with cloned cells and a three times plaque-purified FMDV, C-S8c1 (8). After serial passage of C_1-BHK-Rc1, the cells became increasingly resistant to the parental FMDV C-S8c1, and the resident virus, in turn, evolved to be hypervirulent for BHK-21 cells (9–11). The persistently infected cells can be cured of any detectable FMDV RNA by ribavirin treatment (7, 11) or become spontaneously cured after more than 100 passages in culture. Viruses produced by carrier cultures are designated with R followed by the cell passage number (e.g., R100 is FMDV from C_1-BHK-Rc1 passaged 100 times since the establishment of persistence). The modification of R viruses in the carrier cells was noted by several phenotypic traits: (i) small-plaque morphology, revertible by increasing the DEAE-dextran concentration in the agar overlay (8); (ii) temperature-sensitive (*ts*) character (8); and (iii) instability of virions, with poor recovery of infectivity, and of full-length genomic RNA upon purification of particles. It is not known whether such phenotypic traits are linked and whether they relate to hypervirulence for BHK-21 cells. The instability of R100 virions suggested alterations in the capsid proteins.

Alignment of amino acid sequences of proteins of field isolates of FMDV indicates that amino acid substitutions fixed during viral evolution tend to cluster at defined segments of the viral capsid (18, 32, 44, 45). The three-dimensional structure of FMDV O_1 BFS, elucidated by crystallographic analysis (1) has revealed that such variable regions correspond to exposed loops, some of which are antigenically active domains, as defined by biochemical as well as by immunological methods (2, 13, 39, 48, 52). In particular, a disordered segment on FMDV O_1 BFS matches very closely the main antigenic site of FMDV type C that spans VP1 residues 138 to 156 and that includes a minimum of 10 distinguishable epitopes (33, 34). It was suggested that the hypervariability at this site of FMDV of serotype A was due to increased misincorporation by the FMDV replicase when copying the relevant RNA stretch (58). However, the view that some genomic residues or segments are prone to variation while others must remain invariant is generally based on the analysis of viruses that share a common natural history, for example isolates from acute infections that have been the target of selection by the host immune response (16, 18, 32, 44, 45). Prolonged residence of FMDV in carrier BHK-21 cells offered an entirely new environment to the virus FMDV C-S8c1, one that contrasted with its prior history of acute infections in animals and in cell culture (16).

The analyses reported here show that R100 has fixed several unique amino acids that are not represented in the corresponding position of any FMDV or picornavirus sequenced to date. Some replacements affect positions that were invariant in all previously sequenced FMDVs. In particular, we show that the cysteine at position 7 (C-7) of VP3, which appears to play a key structural role by providing disulfide bridges at the virion fivefold axis (1), is substituted by valine in R100. This and other substitutions fixed in VP1 and VP3 during persistence indicate that, if provided

* Corresponding author.
† Present address: Laboratorio de Modelado Molecular y Química Computacional, UPC, Barcelona, Spain.

with the suitable environment, even genomic positions regarded as highly invariant are subject to rapid change.

MATERIALS AND METHODS

Cells and viruses. The carrier cell line C_1-BHK-Rc1 was established with cloned BHK-21 cells and a three times plaque-purified FMDV C-S8c1, as described previously (8). The viruses rescued from C_1-BHK-Rc1, termed R, were amplified from about 10^6 to 10^9 PFU by infection of BHK-21 cells, using standard procedures (16). The methods for culturing cells and the FMDV infectivity assays have been previously described (8, 16, 43).

FMDV purification. The standard purification of FMDV C-S8c1 involved (i) clarification of the culture medium by centrifugation (3,000 × *g*, 5 min) and shaking with 2% chloroform followed by a second centrifugation (10,000 × *g*, 15 min, 4°C); (ii) addition of EDTA to 5 mM and pelleting of the virus (95,000 × *g*, 3 h, 4°C) through a cushion of 20% sucrose in 10 mM Tris hydrochloride (pH 7.5)–0.1 M NaCl–1 mM EDTA (TNE); (iii) suspension of the pellet in TNE and sedimentation through a 7.5 to 30% sucrose gradient in the same buffer (160,000 × *g*, 70 min, 4°C). The viral protein profile of each gradient fraction was analyzed by sodium dodecyl sulfate (SDS) (0.1%)-polyacrylamide (11%) gel electrophoresis (SDS-PAGE) (29), including 8 M urea. Fractions containing virus were pooled and used either for immunological assays (36) or for extraction of genomic RNA (16). Use of this purification procedure for R100 resulted in about 100-fold decrease in the recovery of infectivity or of viral components, compared with an identical scheme for FMDV C-S8c1. A 10-fold improvement in the yield of R100 was attained by suspending the viral pellet of step ii in cell culture medium (Dulbecco modification of Eagle medium [DMEM]) and using 10 mM Tris hydrochloride (pH 7.5)–1.5 M NaCl as the buffer for sucrose gradient fractionation. Such sedimentation at high ionic strength is suitable for the purification of both FMDV C-S8c1 and R100.

Purification and sequencing of VP3. Capsid protein VP3 of FMDV C-S8c1 and R100 was purified by affinity chromatography as follows. Viral pellets from purification step ii (described above) were suspended in 80 mM Tris hydrochloride (pH 8.0)–2% SDS–5% β-mercaptoethanol and heated at 90°C for 3 min. Then the preparations were diluted in 8 ml of phosphate-buffered saline containing 1% Triton X-100 and chromatographed through Sepharose 4B coupled to monoclonal antibody (MAb) 6C3, specific for VP3 (36). VP3 was eluted with 50 mM diethylamine, pH 11.5. The protein was at least 90% pure as judged by SDS-PAGE. Then, VP3 (4 μg) was electrophoresed in SDS-PAGE (29) and the protein band was transferred to nitrocellulose paper (19), mounted in the reaction chamber of a pulse-phase sequenator (model 477A; Applied Biosystems), and subjected to eight cycles of automated Edman degradation (26, 54).

Immunological assays. The MAbs used in the present study as well as the immunological assays, neutralization of infectivity, enzyme-linked immunoelectrotransfer blot (EITB), and immunodot (EID), have been described previously (34–36).

Molecular cloning and nucleotide sequencing. The first strand of a cDNA copy of the P1 RNA segment of R100 was synthesized as described previously (55) by using as a primer an oligonucleotide complementary to nucleotides 2227 to 2246 (mapping in the 2A/2B-coding region; numbering of nucleotides as in Fig. 1). The second cDNA strand was synthesized by using RNase H as described by Lapeyre and Amalric (30). The cDNA was cloned in plasmid pUC18, and positive transformants were selected by hybridization to specific oligonucleotides, using previously described procedures (12, 42). DNA was sequenced by primer extension and dideoxy chain termination, using T7 DNA polymerase or Sequenase (28, 51). Each nucleotide was read an average of two to three times, and the sequences were processed using the programs developed by Staden (46). In addition, viral RNA was sequenced using dideoxynucleotides and reverse transcriptase, as described previously (45, 59). Sequencing of R100 RNA produced many ambiguities in the sequencing gels (perhaps because of lower average molecular weight of the RNA template), a few of which were resolved by treating the reaction mixtures with terminal deoxynucleotidyl transferase (6).

Molecular modeling studies. The putative hydrophobic pore defined by VP3 of R100 was modeled by a set of five tripeptide chains Ala-Val-Ser (abbreviated AVS; throughout the text the single-letter amino acid code will be used) blocked with *N*-acetyl and *N'*-methylamide at the N and C termini, respectively. The blocked tripeptide mimicks the corresponding sequence within the protein chain. The five chains were aligned parallel, and each one was placed at the vertex of a regular pentagon. The energy of the system was evaluated by molecular mechanics, using the ECEPP/2 force field (37). The energy was minimized by varying the dihedral angles of all peptide chains, as well as the distances between them, while preserving the fivefold symmetry. Starting conformations for minimization were selected by combining preferred dihedral angle values, taken (i) from Ramachandran plots, (ii) from minimum energy structures identified from a similar set of calculations carried out on the simpler model of five blocked valines, or (iii) from random generation of the dihedral angles.

RESULTS

Unique amino acid substitutions in the capsid proteins of R100. FMDV R100, the virus rescued after 100 passages of the carrier C_1-BHK-Rc1 cells (8, 11), showed considerable instability during purification by standard procedures (see Materials and Methods). This was not due to differences of

FIG. 1. Nucleotide sequences of the P1 regions of FMDV C-S8c1 and R100 (VR100). Only residues of R100 that differed from the corresponding ones in C-S8c1 are indicated. The arrows delimit the coding region for each protein (5, 21). Sequences have been determined on cloned cDNA and RNA as detailed in Materials and Methods. The symbol T is used instead of U. Sequence differences between cDNA and RNA were: C-S8c1, residue 812 was C in cDNA and A/C (two bands) in RNA, residue 1135 was C in cDNA and T in RNA, and residue 1764 was C in cDNA and T in RNA; R100, residue 144 was C in cDNA and T in RNA and residue 812 was C in cDNA and A/C (two bands) in RNA. The C-S8c1 RNA sequence reported here differs from that previously determined by Sobrino et al. (44) (who used a viral preparation originated from the same initial stock, C-S8c1, but with a different passage history in cell culture) in positions 292, 477, 543, 612, 812, and 1426 that were G, C, C, C, A, and A, respectively, in the previous report (44). Mutations leading to amino acid substitutions were: VP2, G-829→A (A-182→T), G-832→A (G-183→S); VP3, T-928→G, G-929→T (C-7→V), A-935→C (D-9→A), A-946→C (N-13→H), A-949→T (M-14→L); VP1, A-1813→G (T-83→A), C-2009→A (T-148→K), G-2147→A (G-194→D). Amino acid residues (given in parentheses) are numbered for each individual protein.

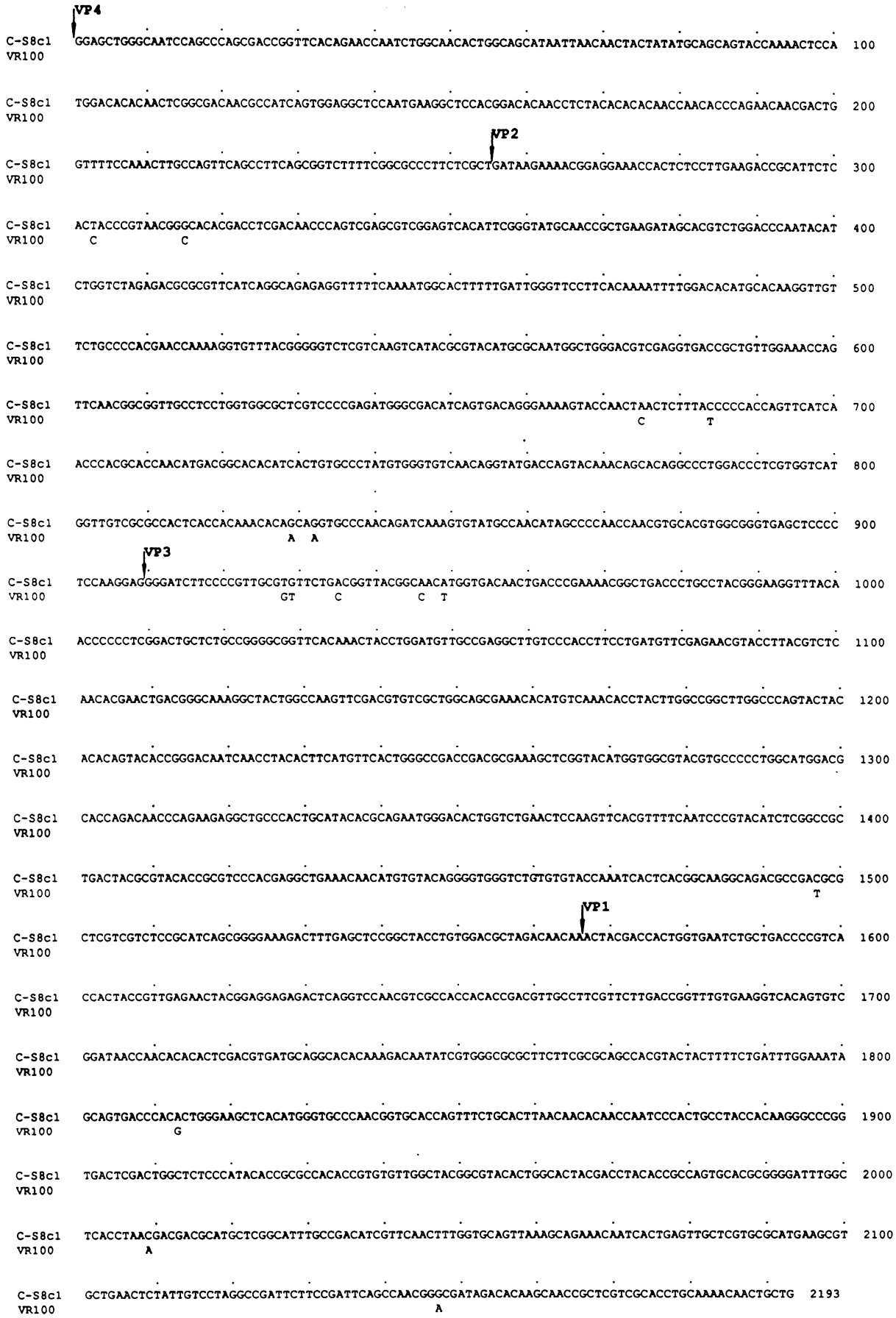
VP4
C-S8c1 GGAGCTGGGCAATCCAGCCCAGCGACCGGTTCACAGAACCAATCTGGCAACACTGGCAGCATAATTAACAACTACTATATGCAGCAGTACCAAAACTCCA 100
VR100
C-S8c1 TGGACACACAACTCGGCGACAACGCCATCAGTGGAGGCTCCAATGAAGGCTCCACGGACACAACCTCTACACACACAACCAACACCCAGAACAACGACTG 200
VR100
VP2
C-S8c1 GTTTTCCAAACTTGCCAGTTCAGCCTTCAGCGGTCTTTTCGGCGCCCTTCTCGCTGATAAGAAAACGGAGGAAACCACTCTCCTTGAAGACCGCATTCTC 300
VR100
C-S8c1 ACTACCCGTAACGGGCACACGACCTCGACAACCCAGTCGAGCGTCGGAGTCACATTCGGGTATGCAACCGCTGAAGATAGCACGTCTGGACCCAATACAT 400
VR100 C C
C-S8c1 CTGGTCTAGAGACGCGCGTTCATCAGGCAGAGAGGTTTTTCAAAATGGCACTTTTTGATTGGGTTCCTTCACAAAATTTTGGACACATGCACAAGGTTGT 500
VR100
C-S8c1 TCTGCCCCACGAACCAAAAGGTGTTTACGGGGGTCTCGTCAAGTCATACGCGTACATGCGCAATGGCTGGGACGTCGAGGTGACCGCTGTTGGAAACCAG 600
VR100
C-S8c1 TTCAACGGCGGTTGCCTCCTGGTGGCGCTCGTCCCCGAGATGGGCGACATCAGTGACAGGGAAAAGTACCAACTAACTCTTTACCCCCACCAGTTCATCA 700
VR100 C T
C-S8c1 ACCCACGCACCAACATGACGGCACACATCACTGTGCCCTATGTGGGTGTCAACAGGTATGACCAGTACAAACAGCACAGGCCCTGGACCCTCGTGGTCAT 800
VR100
C-S8c1 GGTTGTCGCGCCACTCACCACAAACACAGCAGGTGCCCAACAGATCAAAGTGTATGCCAACATAGCCCCAACCAACGTGCACGTGGCGGGTGAGCTCCCC 900
VR100 A A
VP3
C-S8c1 TCCAAGGAGGGGATCTTCCCCGTTGCGTGTTCTGACGGTTACGGCAACATGGTGACAACTGACCCGAAAACGGCTGACCCTGCCTACGGGAAGGTTTACA 1000
VR100 GT C C T
C-S8c1 ACCCCCCTCGGACTGCTCTGCCGGGGCGGTTCACAAACTACCTGGATGTTGCCGAGGCTTGTCCCACCTTCCTGATGTTCGAGAACGTACCTTACGTCTC 1100
VR100
C-S8c1 AACACGAACTGACGGGCAAAGGCTACTGGCCAAGTTCGACGTGTCGCTGGCAGCGAAACACATGTCAAACACCTACTTGGCCGGCTTGGCCCAGTACTAC 1200
VR100
C-S8c1 ACACAGTACACCGGGACAATCAACCTACACTTCATGTTCACTGGGCCGACCGACGCGAAAGCTCGGTACATGGTGGCGTACGTGCCCCCTGGCATGGACG 1300
VR100
C-S8c1 CACCAGACAACCCAGAAGAGGCTGCCCACTGCATACACGCAGAATGGGACACTGGTCTGAACTCCAAGTTCACGTTTTCAATCCCGTACATCTCGGCCGC 1400
VR100
C-S8c1 TGACTACGCGTACACCGCGTCCCACGAGGCTGAAACAACATGTGTACAGGGGTGGGTCTGTGTGTACCAAATCACTCACGGCAAGGCAGACGCCGACGCG 1500
VR100 T
VP1
C-S8c1 CTCGTCGTCTCCGCATCAGCGGGGAAAGACTTTGAGCTCCGGCTACCTGTGGACGCTAGACAACAAACTACGACCACTGGTGAATCTGCTGACCCCGTCA 1600
VR100
C-S8c1 CCACTACCGTTGAGAACTACGGAGGAGAGACTCAGGTCCAACGTCGCCACCACACCGACGTTGCCTTCGTTCTTGACCGGTTTGTGAAGGTCACAGTGTC 1700
VR100
C-S8c1 GGATAACCAACACACACTCGACGTGATGCAGGCACACAAAGACAATATCGTGGGCGCGCTTCTTCGCGCAGCCACGTACTACTTTTCTGATTTGGAAATA 1800
VR100
C-S8c1 GCAGTGACCCACACTGGGAAGCTCACATGGGTGCCCAACGGTGCACCAGTTTCTGCACTTAACAACACAACCAATCCCACTGCCTACCACAAGGGCCCGG 1900
VR100 G
C-S8c1 TGACTCGACTGGCTCTCCCATACACCGCGCCACACCGTGTGTTGGCTACGGCGTACACTGGCACTACGACCTACACCGCCAGTGCACGCGGGGATTTGGC 2000
VR100
C-S8c1 TCACCTAACGACGACGCATGCTCGGCATTTGCCGACATCGTTCAACTTTGGTGCAGTTAAAGCAGAAACAATCACTGAGTTGCTCGTGCGCATGAAGCGT 2100
VR100 A
C-S8c1 GCTGAACTCTATTGTCCTAGGCCGATTCTTCCGATTCAGCCAACGGGCGATAGACACAAGCAACCGCTCGTCGCACCTGCAAAACAACTGCTG 2193
VR100 A

TABLE 1. Amino acid replacements in FMDV R100 and representation of the amino acids in other picornaviruses

Protein	Replacement[a]	Amino acid in FMDV[b]	Amino acid in other picornaviruses[c]	Acceptability[d]
VP1	T-83	C_1, C_3, Asia1, SAT3	Cox (B1, B3, B4) BEV, Rhino (2, 49)	
	↓			5
	A-83	NR	Theiler's ME BeAn, a	
	T-148	C_1	NR	
	↓			4
	K-148	MAR mutant[e]	NR	
	G-194	C_1, C_3, SAT1, 2	Polio (1, 2, 3), Cox A21	
	↓			4
	D-194	NR	NR	
VP2	A-192	C_1	NR	
	↓			5
	T-192	A10, A12	Cox A21, Rhino (1a, 1b)	
	G-193	C_1, O_1K, SAT3	Rhino 89	
	↓			5
	S-193	NR	Theiler's ME (BeAn, GD7, Da) Polio (1, 2, 3), Cox (A21, B1, B3) Rhino (1a, 1b)	
VP3	C-7	All sequenced	NR	
	↓			2
	V-7	NR	Theiler's ME (BeAn, GD7, Da)	
	D-9	All sequenced	NR	
	↓			4
	A-9	NR	NR	
	N-13	C_1	HA (LA, Cr326, Hm175, Mbb)	
	↓			4
	H-13	NR	NR	
	M-14	C_1	NR	
	↓			5
	L-14	A10, A12, O_1K	NR	

[a] All substitutions (with indication of each amino acid and its position in the relevant protein) between C-S8c1 and R100 are included (Fig. 1).

[b] FMDV that included at the corresponding position (38) the amino acid given on the same line. NR, not represented in any FMDV previously analyzed (18, 38).

[c] Picornaviruses (other than FMDV) with amino acids that correspond (38) to the amino acid given on the same line are indicated. Abbreviations: Cox, coxsackievirus; BEV, bovine enterovirus; Rhino, rhinovirus; ME, murine encephalomyelitis virus; Polio, poliovirus; HA, hepatitis A virus. Serotypes and strains follow the accepted nomenclature. Serotypes, subtypes, or isolates of a given picornavirus are in parentheses. NR, not represented in any picornavirus (other than FMDV) previously analyzed (38).

[d] Degree of acceptability (from 0 to 6, with the latter value representing a replacement by the same amino acid) according to Feng et al. (20).

[e] T-148→K was fixed as an accompanying replacement upon passage of a MAb-resistant (MAR) mutant of FMDV C-S8c1 (M. A. Martínez, unpublished results).

titer or in the PFU-to-particle ratio in the initial preparations of FMDV C-S8c1 and R100. Also, careful analysis of fractions from sucrose gradients after various times of sedimentation suggested that the loss of R100 was not due to aggregation of virions but rather to their instability during purification (results not shown). To investigate possible alterations of the viral capsid, the nucleotide sequence of the P1 RNA segment of R100 was determined and aligned with the corresponding region of the parental FMDV C-S8c1 (Fig. 1). All mutations reported in R100 were found both in cDNA and RNA, except the substitutions at positions 935 and 946 that could not be unambiguously read by RNA sequencing. At those positions, three independently derived cDNA clones yielded an identical sequence. A few differences between the sequences determined on cDNA and on RNA were detected that could be due either to heterogeneity in the RNA population or to misincorporations by the reverse transcriptase (Fig. 1). FMDV C-S8c1 and R100 differ in 15 point mutations, 7 transitions and 8 transversions. The deduced amino acid sequences indicate nine substitutions, two located in VP2, four in VP3, and three in VP1. Five substitutions (T-83→A in VP1 and the four at the N-terminal segment of VP3) clustered around the fivefold axis of FMD virions (1). In particular, C-7 of VP3, which with F-3 and V-5 delimit a hydrophobic pore at the fivefold axis (1), is substituted by V in R100 (Fig. 1, Table 1). To ascertain that mature R100 virions included V at position 7, VP3 proteins from FMDV C-S8c1 and R100 were purified by affinity chromatography and their N-terminal residues were sequenced by automated Edman degradation. The sequences found were XIFPVAXS for C-S8c1 and, XIFPVAVS for R100. (The analytical procedure used does not allow determination of G or underived C, and these positions are indicated as X.) The result confirms the presence of V-7 in VP3 of R100 and shows, in addition, that despite a cluster of substitutions near the N terminus of VP3, the proteolytic processing at the VP2/VP3 junction occurred at the expected E/G doublet.

Analysis of the three-dimensional structure of FMDV O_1 BFS (1) and unpublished biochemical evidence quoted in reference (1) suggest that at the fivefold axes, the C-7 residues of some of the five VP3 molecules in each pentamer are involved in covalent linkage of VP3 pairs by disulfide bonds (1). To test whether the latter were present in FMDV C-S8c1 and absent in R100, EITB assays were carried out by using specific MAbs after disruption of C-S8c1 and R100 under reducing and nonreducing conditions (Fig. 2). Upon heating of virions in the presence of β-mercaptoethanol, only the monomeric forms of VP3 of C-S8c1 and R100 were detected. However, under nonreducing conditions, C-S8c1 included dimeric (bands at 48 and 52 and minor forms) and

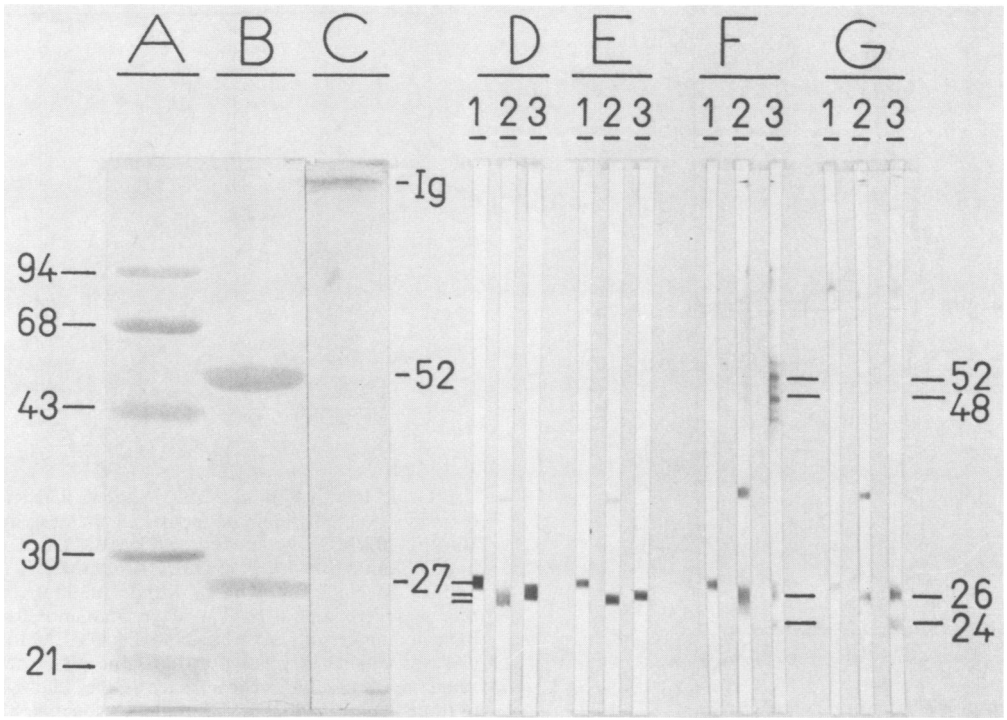

FIG. 2. EITB assays with FMDV C-S8c1 and R100 disrupted under reducing or nonreducing conditions. The samples applied to each lane were: A, molecular size markers; B and C, purified MAb 6F6 (stained with amido black after transfer to nitrocellulose); D and F, FMDV C-S8c1; E and G, FMDV R100. Both viruses were purified through step ii, as described in Materials and Methods. Samples were disrupted with SDS in the presence of β-mercaptoethanol and heated (lanes A, B, D, and E) or treated with SDS in the absence of β-mercaptoethanol (lanes C, F, and G). Electrophoresis was by the method of Laemmli (29). The immunoreaction was carried out with a mixture of: MAbs 3E5, 6D11, and SC9, directed against VP1 (lanes 1); MAb 4A3, anti-VP2 (lanes 2); MAbs 6F6 and 6C3, anti-VP3 (lanes 3). The MAbs have been previously characterized (33–36). The minor band in lanes 2 is a contaminating protein that reacts with MAb 4A3. A diminished reactivity with MAbs of samples not treated with β-mercaptoethanol was observed and was probably due to incomplete disruption and electrotransfer of virions; heating did not influence the band patterns (results not shown). Numbers pointing to bands indicate molecular sizes in kilodaltons.

monomeric (bands at 24 and 26) VP3, whereas R100 showed only monomeric VP3 (Fig. 2, lanes F3 and G3). The different bands in C-S8c1 may reflect conformational states affected by the presence or absence of a putative disulfide bridge between C-178 and C-184 located at the VP3 G-H loop (1). Other C residues, 183 of VP1, 120 of VP2, and 7, 51, and 141 of VP3, are probably not located at positions adequate to form intramolecular disulfide bonds (1). No bands corresponding to VP heterodimers, reactive with two MAbs directed to different capsid proteins, were detected (Fig. 2). Thus, the result is that expected from participation of C-7 of VP3 in disulfide bridges to produce dimeric forms of VP3 and from the replacement of C-7 by V-7 in R100.

Density in cesium chloride and sensitivity to photoinactivation by intercalating dyes of R100. FMDV has a higher buoyant density in cesium chloride and sensitivity to photoinactivating dyes than other picornaviruses (41). Such properties have been explained by the penetration of ions or dye molecules through the pore at the fivefold axis (1). Since some replacements in R100 affected VP3 segments involved in delimiting such a hydrophobic pore, it was interesting to test whether FMDV C-S8c1 and R100 differed in density in cesium chloride and in sensitivity to photoinactivation by neutral red (3-amino-7-dimethylamino-2-methylphenazine hydrochloride). Figure 3 shows the infectivity profiles of FMDV C-S8c1 and R100 after sedimentation in a cesium chloride density gradient. For both viruses, 90% of the infectivity banded within the range of densities of 1.43 to 1.50 g/cm^3, with a peak at 1.454 ± 0.016 g/cm^3 for C-S8c1 (average of five determinations) and at 1.494 ± 0.007 g/cm^3 for R100 (four determinations). No bands of infectivity were seen at densities below 1.43 g/cm^3. Thus, R100 shows the high density in cesium chloride typical of aphthoviruses, compatible with free penetration of cesium ions into the viral particles (1, 41).

The photoinactivation of FMDV C-S8c1 and R100 was studied at low and high ionic strengths. Even though the rate of inactivation varied somewhat depending on the medium used, no significant differences were noted between C-S8c1 and R100 (Fig. 4). The result suggests that the dye had no impediment to reach the target R100 RNA (1, 41).

Altered antigenicity of R100. The replacements fixed on VP1 and VP2 of R100 are located on exposed loops, according to predictions derived from the alignment of the FMDV proteins with those of human rhinovirus 14 and mengo virus (aided by three-dimensional superposition [31]) and from the atomic structure of FMDV O_1 BFS (1). Substitutions T-148→K and G-194→D were sequentially fixed in R in the course of persistence (11) and are located at the main antigenic loop of FMDV type C (residues 138 to 150) and at the C-terminal segment of VP1, respectively. Both domains are involved in neutralizing and protective immune responses in animals (2, 13, 18, 34, 39, 48). To test whether the two substitutions affected the antigenicity of FMDV, the reactivity of C-S8c1, R19, which included T-148→K as the sole replacement in VP1, R58, with both T-148→K and

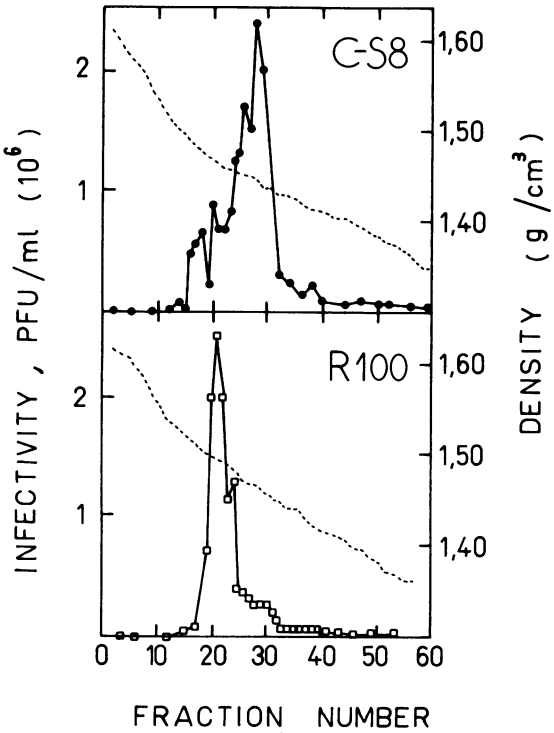

FIG. 3. Infectivity profiles upon banding FMDV C-S8c1 and R100 in a cesium chloride density gradient. FMDV from purification step ii (see Materials and Methods) were suspended in DMEM, adjusted to a cesium chloride density of 1.46 g/cm^3 (volume, 11 ml) by refractometry (calibrated with cesium chloride solutions of known density measured by pycnometry), clarified by a brief high-speed ultracentrifugation, and then run at 28,000 rpm for 72 h at 4°C in an SW40 rotor. The refractive index of each fraction was measured to determine the gradient profile (discontinuous line). Samples of the indicated fractions were diluted in DMEM and titrated. A portion of each fraction was applied to nitrocellulose, and EID assays were carried out with MAb SD6 (reactive with C-S8c1 and R100) and MAb 4G3 (specific for C-S81; see Table 2 for the origin of MAbs). The EID profiles in all cases gave the expected reactivities, and the profiles paralleled those of infectivity. Banding of virus purified through step iii (sucrose gradient at high ionic strength followed by dialysis against DMEM; see Materials and Methods) resulted in similar infectivity profiles but with noninfectious viral protein at the top of the gradients detected by EID assays (results not shown).

G-194→D, and R100 were assayed with a panel of 15 MAbs that recognize VP1, VP2, or VP3 (34–36). In EITB assays, a significant decrease of the reactivity of VP1 or VP2 of R was noted with some of the MAbs (Table 2). The epitope recognized by MAb SD6 has been mapped at residues 138, 139, 146, and 147, and that recognized by MAb 4G3 has been mapped at residues 146 and 148 to 150 of VP1 (34, 35). The binding of SD6 to VP1 of each FMDV R tested was indistinguishable from that to C-S8c1. Interestingly, however, the neutralization of either R58 or R100 by SD6 was about 10^3-fold less effective than that of R19 or C-S8c1, suggesting an effect of other substitutions in determining viral neutralization (see Discussion). None of the R viruses was neutralized by MAb 4G3, as expected from the absence of binding to the substituted VP1 (Table 2). Thus, antigenic variants of FMDV were selected in the course of persistence in BHK-21 cells, in the absence of antibodies.

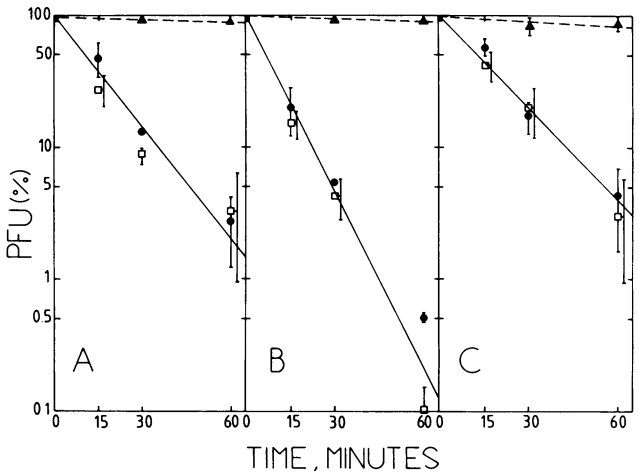

FIG. 4. Inactivation of FMDV C-S8c1 and R100 by neutral red (3-amino-7-dimethylamino-2-methylphenazine hydrochloride). About 10^5 PFU of FMDV was mixed with DMEM (A), DMEM–50 mM Tris hydrochloride (pH 7.6) (B), DMEM–50 mM Tris hydrochloride (pH 7.6)–1.5 M NaCl (C), with or without neutral red (10 μg/ml). The mixtures were kept at 22°C at 70 cm from an F30w, cw lamp. At the indicated times, aliquots were diluted in DMEM and plated. The PFU (%) was calculated relative to the same virus incubated during the same time period but in the absence of dye. Each value is the average of three determinations in different experiments. Significant standard deviations are indicated. Symbols: ●, C-S8c1; □, R100; ▲, encephalomyocarditis virus.

DISCUSSION

The analysis of the capsid proteins of FMDV after prolonged persistence in BHK-21 cells has revealed substitutions at one conformationally important domain around the fivefold axis of the particle and at exposed loops that result in altered viral reactivity with neutralizing MAbs. Substitutions G-194→D in VP1 and D-9→A and N-13→H in VP3 result in amino acids that, upon sequence alignment, are not represented in the corresponding positions of any picornavirus sequenced to date (18, 38); T-148→K has been identified in a MAb-resistant mutant of FMDV C-S8c1 (Table 1). It was particularly striking that C-7 of VP3 was substituted by V in R100, since C-7 provides disulfide bridges at the FMDV fivefold axis and may limit the flexibility of the rim of a hydrophobic pore (1). Generally, cysteines contribute to the stabilization of folded protein structures (40) and are highly conserved among homologous proteins. C-7 of VP3 has been found in all aphthoviruses sequenced to date (38), R100 being, to our knowledge, the first exception. Although the absence of disulfide bridges at the fivefold axis of R100 may contribute to the observed instability of the virus, our molecular modeling studies suggest that the hydrophobic pore configuration can be preserved by the arrangement of five valyl residues which show a tendency to remain associated. More specifically, after exploration of the multidimensional energy hypersurface, all low-energy structures reveal the tendency of the polypeptide chains to give rise to a pore formation, with valyl side chains pointing toward the interior of the hydrophobic pore. Furthermore, after discarding a few of these structures (see below), the remaining ones tend to be closely related, showing a similar value for the interchain distance. In addition, they all depict the hydrophobic valine side chains directed toward the interior of the pore.

Relevant energy and conformational parameters pertain-

TABLE 2. Reactivity of MAbs with capsid proteins of FMDV C-S8c1, R19, R58, and R100 in EITB assays

MAb[a]	Protein recognized	Reactivity of MAbs with antigen[b]			
		C-S8c1	R19 (T-148→K)[c]	R58 (T-148→K), (G-194→D)[c]	R100 (T-148→K), (G-194→D), (T-83→A)[c]
SB3	VP1	+	+	+	+
SD6	VP1	+	+	+	+
4G3	VP1	+	−	−	−
7CA8	VP1	+	+	+	+
7JD1	VP1	+	+	+	+
7CA11	VP1	+	+	+	+
7FC12	VP1	+	+	±	±
7AH1	VP1	+	+	±	±
7EE6	VP1	−	ND	ND	−
6EE2	VP1	+	+	+	+
6F2	VP2	+	+	±	±
4A3	VP2	+	+	+	+
6F6	VP3	+	+	+	+
6C3	VP3	+	+	+	+
6C2	VP3	+	+	+	+

[a] The antigens used to produce the MAbs employed in this study were: FMDV C-S8c1 (MAbs SB3, SD6, 4G3, 6F2, 6F6, 6C3, and 6C2), C_3-Indaial (MAbs 7CA8, 7JD1, 7CA11, 7FC12, 7AH1, and 7EE6), C_1-Brescia (MAb 4A3), and A_{12} (MAb 6EE2). Their properties have been described previously (34–36).

[b] The FMDV used as antigens and the EITB assay are described in Materials and Methods. Symbols denote reactivity of the MAbs relative to that with FMDV C-S8c1 (except for MAb 7EE6, taken relative to C_3-Indaial). +, reactivity indistinguishable from that with C-S8c1; −, at least 50-fold lower than that with C-S8c1; ±, 2- to 10-fold lower. Equal amounts of antigen (2 μg of VP1) were used, as quantitated by densitometry of Coomassie blue-stained electropherograms and of EID assays with a mixture of reactive MAbs.

[c] The amino acid differences between VP1 of the R viruses and that of C-S8c1, which were sequentially fixed during persistence (11), are given in parentheses.

ing to the 10 lowest energy structures identified are shown in Table 3. Structures 1 and 9 are disregarded for the present discussion, because they represent structures unlikely to occur if the tripeptide were part of a protein chain. Indeed, their stabilization is due to hydrogen bonds which prevent the five chains from aligning in a parallel fashion. The rest of the structures show a high interchain stabilization energy, and the isolated chains show relatively high conformational energies. Consequently, the calculations suggest a high tendency for the chains to stick together because of high stabilization energy upon association. Figure 5 top depicts the structure corresponding to minimum 2 in Table 3. The structures exhibit an average distance between Cα atoms of adjacent valyl residues of about 0.65 nm, comparable with the 0.7 nm found in the X-ray structure of FMDV O_1 BFS (1).

Furthermore, the average distance between two Hγs of the side chain located on the plane of the pore of two adjacent valine residues is about 0.34 nm compared with the 0.36-nm intersulfide distances observed in the crystal structure. In summary, the hydrogens of the side chains of valine delimit a pore whose diameter is about 0.58 nm, which compares well with the value of 0.6 nm determined from the X-ray structure (1) and is consistent with the free penetration of neutral red in both C-S8c1 and R100 (Fig. 4), since the dye can be modeled for these considerations as a parallelepiped of about 0.55-nm width (Fig. 5). Likewise, the modeling studies suggest free penetration of cesium ions (diameter, 0.33 nm; 57) into C-S8c1 and R100 (Fig. 3). Also, the increase in hydrophobic interactions that will occur among the V side chains at high ionic strength provides an interpretation for the improved recovery of R100 in sucrose gradients with 1.5 M NaCl (see Materials and Methods).

The net gain of positive charges at the N-terminal segment of VP3 that was brought about by substitutions D-9→A and N-13→H (Table 1) may also contribute to the instability of R100. This VP3 segment, located at a shallow depression around the fivefold axis, is juxtaposed to a VP1 stretch around position 83, which is also substituted in R100, and, thus, the amino acid replacements may affect the pentameric VP1-VP3 interaction (see Fig. 4b in reference 1). An evaluation of the effect of such amino acid replacements on FMDV serotype C would require modeling of the entire fivefold axis domain. When the atomic coordinates of FMDV O_1 BFS (1) become available, modeling of FMDV C-S8c1 will be attempted to assess more precisely the structural implications of the substitutions fixed in R100.

The C-7→V replacement required two transversions (U-928→G and G-929→U; see Fig. 1) to occur. These mutations separately would lead to C-7→G and C-7→F, respectively, both with a degree of acceptability slightly higher than C→V

TABLE 3. Energy minimization of five tripeptide (AVS) chains with fivefold symmetry[a]

Structure no.	E_{tot}[b]	E_{chain}[c]	ΔE[d]	d[e]	Dihedral angles (°)[f]							
					φ2	ψ2	φ3	ψ3	φ4	ψ4	χ42	φ5
1	−71.1	0.6	−74.1	0.84	−74	135	−70	−24	−93	−3	71	−44
2	−52.5	−0.1	−51.9	0.60	−114	78	−145	140	−160	82	55	−167
3	−39.8	2.6	−53.0	0.67	−71	−44	−144	31	−72	−68	177	179
4	−39.8	2.6	−53.0	0.67	−71	−44	−144	31	−72	−68	177	−62
5	−35.8	1.7	−44.5	0.54	−151	177	−59	−29	−155	151	−179	180
6	−34.3	3.0	−49.2	0.66	−70	−45	−143	31	−72	−54	92	−59
7	−34.3	3.0	−49.2	0.67	−70	−46	−143	31	−74	−54	93	61
8	−30.0	2.1	−40.5	0.72	−123	70	−146	142	−163	141	64	−69
9	−27.3	0.2	−28.4	0.88	−70	116	−62	139	−150	80	54	53
10	−20.1	2.1	−30.7	0.67	−134	158	−151	141	−161	160	75	55

[a] The procedure used is described in Materials and Methods. The 10 structures correspond to the 10 lowest minima found for five parallel chains of AVS blocked with *N*-acetyl and *N'*-methylamide at the N and C termini, respectively.

[b] Total conformational energy in kilocalories per mole.

[c] Conformational energy per isolated chain in kilocalories per mole.

[d] Conformational interaction energy ($\Delta E = E_{tot} - 5E_{chain}$) in kilocalories per mole.

[e] $d(C\alpha_i - C\alpha_{i+1})$ corresponds to the distance between the alpha carbon of two valines in adjacent chains expressed in nanometers.

[f] After minimization, some of the angles had the same value for all the identified structures and are not shown here. Values for these angles are: ψ1, ~60°; ω1, ~180°; ω2, ~180°; χ2, ~60°; ω3, ~180°; χ31, ~70°; χ32 and χ33, ~60°; ω4, ~180°; χ41, ~60°.

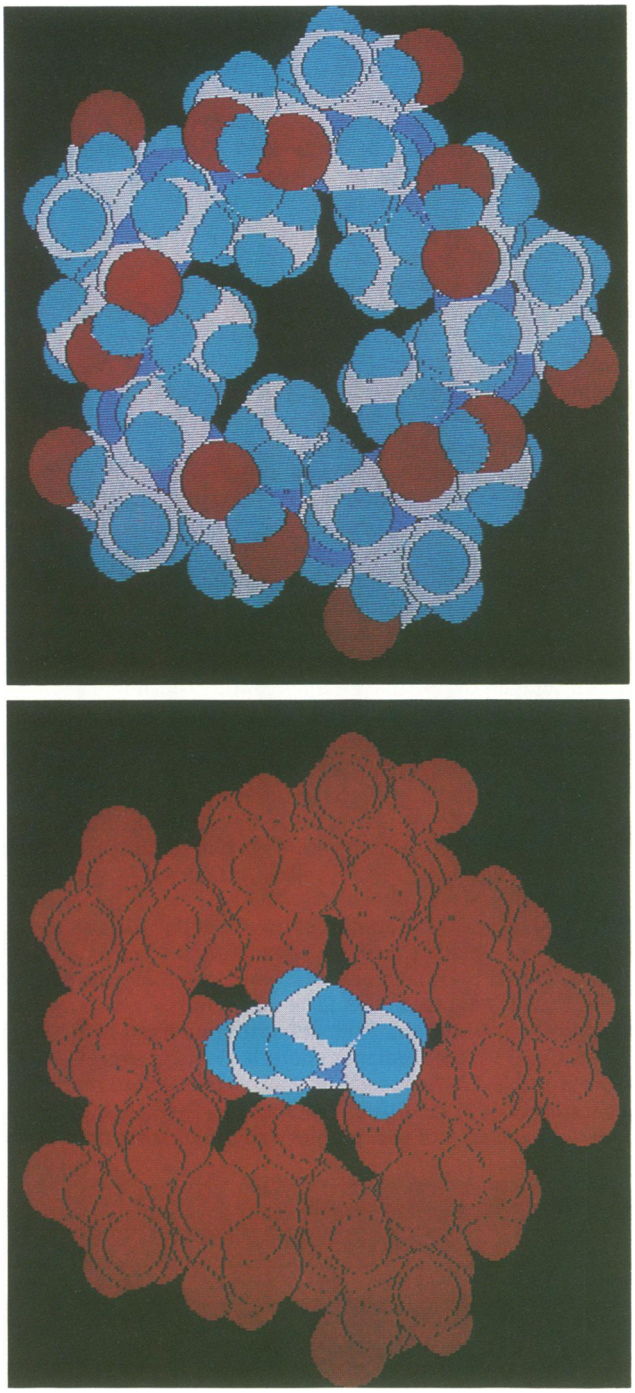

FIG. 5. (Top) Model of the hydrophobic pore formed by association of five parallel tripeptide chains of AVS blocked at the N and C termini with *N*-acetyl and *N'*-methylamide, respectively. C, N, O, and H are shown in white, blue, red, and light blue, respectively. (Bottom) A neutral red dye molecule is shown docked inside the modeled R100 hydrophobic pore (shown in red). Plots were carried out by using the Alchemy program (Tripos Associates, Inc.).

(20). We are currently analyzing viruses from early C_1-BHK-Rc1 cell passages to determine whether particles with G-7 or F-7 in VP3 were transiently present. Of the 15 mutations fixed in P1 of R100, only 5 were silent (Fig. 1). In contrast, among viruses related to FMDV C-S8c1 which were isolated from acute episodes of disease in the field, more than 75% of the mutations in P1 RNA (44) or the polymerase (3D) gene (56) were silent. The reason for this difference, which appears to be statistically significant, is not understood.

Changes in antigenicity of FMDV R100 were revealed by analysis of reactivity with MAbs (Table 2). FMDV R58 and R100 were neutralized less effectively than C-S8c1 and R19 by MAb SD6 despite its similar binding to the four viruses (Table 2) and despite R19, R58, and R100 sharing the same sequence between VP1 residues 133 to 156, where the epitope recognized by MAb SD6 was located (35). It is likely that substitution G-194→D of VP1, present in R58 and R100 but not in C-S8c1 or R19, is responsible for this effect since in the three-dimensional structure of FMDV O_1 BFS the carboxy-terminal stretch of VP1 lies near the main antigenic loop (residues 137 to 156) of the adjacent protomer (1). However, synthetic peptides representing VP1 segment 133 to 156 reacted with MAb SD6 to the same extent as the equivalent molar amount of VP1 in complete virus (35). Also, MAb SD6-resistant mutants of FMDV C-S8c1 showed replacements between residues 138 and 146 but not at the C terminus of VP1 (34, 35). Furthermore, a peptide representing the C terminus of VP1 did not react with MAb SD6 (36). These observations suggest that binding and neutralization sites of MAb SD6 are included within VP1 residues 133 and 156 and that substitution G-194→D impairs in some unknown way virus neutralization. This point is under investigation.

Anti-FMDV antibodies were not involved in the establishment or maintenance of carrier cell cultures (8), nor were they detected in the fetal calf serum used for cell culture (14). Selection of antigenic variants of FMDV in the absence of anti-FMDV antibodies was also observed upon serial passage of FMDV C-S8c1 in cytolytic infections (14), suggesting that it may be a common occurrence due to fluctuations in the quasispecies distribution of genomes (14–18, 27, 35, 43, 47). Bolwell et al. (3) showed that an antigenic variant of FMDV, A22 Iraq 24/64, was selected upon adaptation of the virus to Spinner suspension cultures, an environmental change that is obviously unrelated to immune pressure. Early work by Hampar and Keehn (23) indicated a change in the antigenic properties of herpes simplex virus during persistence in cell culture. These findings provide increasing evidence for the interesting possibility that antigenic variation need not be the result of immune selection. The high mutation rates operating during RNA genome replication (17, 27, 47) facilitate frequent fixation of substitutions at sites at which they are most tolerated, such as exposed loops relatively free of structural constraints, where antigenic sites are commonly located. We are currently sequencing other genomic segments of FMDV R100 and, as expected, substitutions occur at all loci examined (Díez et al., unpublished results). It will not be easy to distinguish in a precise fashion passenger mutations from those that determine genomic fluctuations in viral quasispecies.

ACKNOWLEDGMENTS

We thank M. Medina, E. Martínez-Salas, and J. Avila for help with some experiments and for suggestions and E. Brocchi, D. Morgan, and H. Barahona for supplying MAbs. We are indebted to G. Belsham and M. Medina for indicating to us the N terminus of VP4 of FMDV type C and to A. M. Q. King for suggesting the experiment shown in Fig. 2.

Work at the Centro de Biología Molecular was supported by Comisión Interministerial de Ciencia y Tecnología (grant numbers BIO 88-0452-C05-01 and BIO 89-0668-CO3-O2) and Fundación

Ramón Areces. Work at the Universitat de Barcelona was supported by Comisión Interministerial de Ciencia y Tecnología (grant numbers BT86-0018 and FAR 88-0617). J.D. was supported by a predoctoral fellowship from Consejo Superior de Investigaciones Científicas.

LITERATURE CITED

1. **Acharya, R., E. Fry, D. Stuart, G. Fox, D. Rowlands, and F. Brown.** 1989. The three-dimensional structure of foot-and-mouth disease virus at 2.9 Å resolution. Nature (London) **337**:709–715.
2. **Bittle, J. L., R. A. Houghten, H. Alexander, T. M. Shinnick, J. G. Sutcliffe, R. A. Lerner, D. J. Rowlands, and F. Brown.** 1982. Protection against foot-and-mouth disease by immunization with a chemically synthesized peptide predicted from the viral nucleotide sequence. Nature (London) **298**:30–33.
3. **Bolwell, C., A. L. Brown, P. V. Barnett, R. O. Campbell, B. E. Clarke, N. R. Parry, E. J. Ouldridge, F. Brown, and D. J. Rowlands.** 1989. Host cell selection of antigenic variants of foot-and-mouth disease virus. J. Gen. Virol. **62**:2050–2058.
4. **Burrows, R.** 1966. Studies on the carrier state of cattle exposed to foot-and-mouth disease virus. J. Hyg. **64**:81–90.
5. **Chow, M., J. F. E. Newman, D. Felman, J. M. Hogle, D. J. Rowlands, and F. Brown.** 1987. Myristylation of picornavirus capsid protein VP4 and its structural significance. Nature (London) **237**:482–486.
6. **DeBorde, D. C., V. W. Naeve, L. Herlocher, and H. F. Maassab.** 1986. Resolution of a common RNA sequencing ambiguity by terminal deoxynucletidyl transferase. Anal. Biochem. **157**:275–282.
7. **de la Torre, J. C., B. Alarcón, E. Martínez-Salas, L. Carrasco, and E. Domingo.** 1987. Ribavirin cures cells of a persistent infection with foot-and-mouth disease virus in vitro. J. Virol. **61**:233–235.
8. **de la Torre, J. C., M. Dávila, F. Sobrino, J. Ortín, and E. Domingo.** 1985. Establishment of cell lines persistently infected with foot-and-mouth disease virus. Virology **145**:24–35.
9. **de la Torre, J. C., S. de la Luna, J. Díez, and E. Domingo.** 1989. Resistance to foot-and-mouth disease virus mediated by *trans*-acting cellular products. J. Virol. **63**:2385–2387.
10. **de la Torre, J. C., E. Martínez-Salas, J. Díez, and E. Domingo.** 1989. Extensive cell heterogeneity during a persistent infection with foot-and-mouth disease virus. J. Virol. **63**:59–63.
11. **de la Torre, J. C., E. Martínez-Salas, J. Díez, A. Villaverde, F. Gebauer, E. Rocha, M. Dávila, and E. Domingo.** 1988. Coevolution of cells and viruses in a persistent infection of foot-and-mouth disease virus in cell culture. J. Virol. **62**:2050–2058.
12. **de la Torre, J. C., J. Ortín, E. Domingo, J. DeLamarter, B. Allet, J. Davies, K. P. Bertrand, L. V. Wray, and W. S. Reznikoff.** 1984. Plasmid vectors based on Tn10 DNA: gene expression regulated by tetracycline. Plasmid **12**:103–110.
13. **Di Marchi, R., G. Brooke, C. Gale, V. Cracknell, T. Doel, and N. Mowat.** 1986. Protection of cattle against foot-and-mouth disease by a synthetic peptide. Science **232**:639–641.
14. **Díez, J., M. G. Mateu, and E. Domingo.** 1989. Selection of antigenic variants of foot-and-mouth disease virus in the absence of antibodies, as revealed by an in situ assay. J. Gen. Virol. **70**:3281–3289.
15. **Domingo, E.** 1989. RNA virus evolution and the control of viral disease. Prog. Drug Res. **33**:93–133.
16. **Domingo, E., M. Dávila, and J. Ortín.** 1980. Nucleotide sequence heterogeneity of the RNA from a natural population of foot-and-mouth disease virus. Gene **11**:333–346.
17. **Domingo, E., and J. J. Holland.** 1988. High error rates, population equilibrium and evolution of RNA replication systems, p. 3–36. *In* E. Domingo, J. J. Holland, and P. Ahlquist (ed.), RNA genetics, vol. 3. CRC Press Inc., Boca Raton, Fla.
18. **Domingo, E., M. G. Mateu, M. A. Martínez, J. Dopazo, A. Moya, and F. Sobrino.** 1990. Genetic variability and antigenic diversity of foot-and-mouth disease virus, p. 233–266. *In* E. Kurstak, R. G. Marusyk, F. A. Murphy, and M. H. V. van Regenmortel (ed.), Applied virology research, vol. 2. Plenum Publishing Corp., New York.
19. **Dunn, S. D.** 1986. Effects of the modification of transfer buffer composition and the renaturation of proteins in gels on the recognition of proteins on western blots by monoclonal antibodies. Anal. Biochem. **157**:144–153.
20. **Feng, D. F., M. S. Johnson, and R. F. Doolittle.** 1985. Aligning amino acid sequences: comparison of commonly used methods. J. Mol. Evol. **21**:112–125.
21. **Forss, S., K. Strebel, E. Beck, and H. Schaller.** 1984. Nucleotide sequence and genomic organization of foot-and-mouth disease virus. Nucleic Acids Res. **12**:6587–6601.
22. **Gebauer, F., J. C. de la Torre, I. Gomes, M. G. Mateu, H. Barahona, B. Tiraboschi, I. Bergmann, P. Augé de Mello, and E. Domingo.** 1988. Rapid selection of genetic and antigenic variants of foot-and-mouth disease virus during persistence in cattle. J. Virol. **62**:2041–2049.
23. **Hampar, B., and M. A. Keehn.** 1967. Cumulative changes in the antigenic properties of herpes simplex virus from persistently infected cell cultures. J. Immunol. **99**:554–557.
24. **Hedger, R. S.** 1968. The isolation and characterization of foot-and-mouth disease virus from clinically normal herds of cattle in Botswana. J. Hyg. **66**:27–36.
25. **Hedger, R. S., and B. Condy.** 1985. Transmission of foot-and-mouth disease from African buffalo virus carriers to bovine. Vet. Rec. **117**:205.
26. **Hewick, R. M., M. W. Hunkapiller, L. E. Hood, and J. W. Dreyer.** 1981. A gas-liquid solid phase peptide and protein sequenator. J. Biol. Chem. **256**:7990–7997.
27. **Holland, J. J., K. Spindler, F. Horodyski, E. Grabau, S. Nichol, and S. VandePol.** 1982. Rapid evolution of RNA genomes. Science **215**:1577–1585.
28. **Kraft, R., J. Tardiff, K. S. Franter, and L. A. Leinwand.** 1988. Using mini-prep plasmid DNA for sequencing double stranded templates with sequenase. Biotechniques **6**:544–547.
29. **Laemmli, U. K.** 1970. Cleavage of the structural protein during the assembly of the head of bacteriophage T4. Nature (London) **227**:680–685.
30. **Lapeyre, B., and F. Amalric.** 1985. A powerful method for the preparation of cDNA libraries: isolation of cDNA encoding a 100 Kdal nucleolar protein. Gene **37**:215–220.
31. **Luo, M., M. G. Rossmann, and A. Palmenberg.** 1988. Prediction of three-dimensional models for foot-and-mouth disease virus and hepatitis A virus. Virology **166**:503–514.
32. **Martínez, M. A., C. Carrillo, J. Plana, R. Mascarella, J. Bergadá, E. L. Palma, E. Domingo, and F. Sobrino.** 1988. Genetic and immunogenic variations among closely related isolates of foot-and-mouth disease virus. Gene **62**:75–84.
33. **Mateu, M. G., J. L. Da Silva, E. Rocha, D. L. De Brum, A. Alonso, L. Enjuanes, E. Domingo, and H. Barahona.** 1988. Extensive antigenic heterogeneity of foot-and-mouth disease virus of serotype C. Virology **167**:113–124.
34. **Mateu, M. G., M. A. Martínez, L. Capucci, D. Andreu, E. Giralt, F. Sobrino, E. Brocchi, and E. Domingo.** 1990. A single amino acid substitution affects multiple overlapping epitopes in the major antigenic site of foot-and-mouth disease virus of serotype C. J. Gen. Virol. **71**:629–637.
35. **Mateu, M. G., M. A. Martínez, E. Rocha, D. Andreu, J. Parejo, E. Giralt, F. Sobrino, and E. Domingo.** 1989. Implications of a quasispecies genome structure: effect of frequent, naturally occurring amino acid substitutions on the antigenicity of foot-and-mouth disease virus. Proc. Natl. Acad. Sci. USA **86**:5883–5887.
36. **Mateu, M. G., E. Rocha, O. Vicente, F. Vayreda, C. Navalpotro, D. Andreu, E. Pedroso, E. Giralt, L. Enjuanes, and E. Domingo.** 1987. Reactivity with monoclonal antibodies of viruses from an episode of foot-and-mouth disease. Virus Res. **8**:261–274.
37. **Momany, F. A., L. M. Carruthers, R. F. McGuire, and H. A. Sheraga.** 1974. Intermolecular potentials from crystal data. III. Determination of empirical potentials and application to the packing configurations and lattice energies in crystals of hydrocarbons, carboxylic acids, amines and amides. J. Physical Chem. **78**:1595–1620.
38. **Palmenberg, A.** 1989. Sequence alignments of picornavirus capsid proteins, p. 211–214. *In* B. L. Semler and E. Ehrenfeld

(ed.), Molecular aspects of picornavirus infection and detection. American Society for Microbiology, Washington, D.C.
39. **Pfaff, E., M. Mussgay, H. O. Bohm, G. E. Schulz, and H. Schaller.** 1982. Antibodies against a preselected peptide recognize and neutralize foot-and-mouth disease virus. EMBO J. **7**:869–874.
40. **Richardson, J. S.** 1981. The anatomy and taxonomy of protein structure, p. 167–339. *In* C. B. Anfinsen, J. T. Edsall and F. M. Richards (ed.), Advances in protein chemistry, vol. 34. Academic Press, Inc., New York.
41. **Rueckert, R. R.** 1990. Picornaviridae and their replication, p. 507–548. *In* B. N. Fields and D. M. Knipe (ed.), Virology, vol. 1. Raven Press, New York.
42. **Sambrook, K. J., E. F. Fritsch, and T. Maniatis.** 1989. Molecular cloning: a laboratory manual. Cold Spring Harbor Laboratory, Cold Spring Harbor, N.Y.
43. **Sobrino, F., M. Dávila, J. Ortín, and E. Domingo.** 1983. Multiple genetic variants arise in the course of replication of foot-and-mouth disease virus in cell cultures. Virology **128**:310–318.
44. **Sobrino, F., M. A. Martínez, C. Carrillo, and E. Beck.** 1989. Antigenic variation of foot-and-mouth disease virus of serotype C during propagation in the field is mainly restricted to only one structural protein (VP1). Virus Res. **14**:273–280.
45. **Sobrino, F., E. L. Palma, E. Beck, M. Dávila, J. C. de la Torre, P. Negro, N. Villanueva, J. Ortín, and E. Domingo.** 1986. Fixation of mutations in the viral genome during an outbreak of foot-and-mouth disease: heterogeneity and rate variations. Gene **50**:149–159.
46. **Staden, R.** 1980. A new computer method for the storage and manipulation of DNA gel reading data. Nucleic Acids Res. **8**:3673–3694.
47. **Steinhauer, D., and J. J. Holland.** 1987. Rapid evolution of RNA viruses. Annu. Rev. Microbiol. **41**:409–433.
48. **Strohmaier, K., R. Franze, and K. H. Adam.** 1982. Location and characterization of the antigenic portion of the FMDV immunizing protein. J. Gen. Virol. **59**:295–306.
49. **Sutmoller, P., and A. Gaggero.** 1965. Foot-and-mouth disease carriers. Vet. Rec. **77**:968–969.
50. **Sutmoller, P., J. W. McVicar, and G. E. Cottral.** 1986. The epizootical importance of foot-and-mouth disease carriers. I. Experimentally produced foot-and-mouth disease carriers in susceptible and immune cattle. Arch. Gesamte Virusforsch. **23**:227–235.
51. **Tabor, S., and C. C. Richardson.** 1987. DNA sequence analysis with a modified bacteriophage T7 DNA polymerase. Proc. Natl. Acad. Sci. USA **84**:4767–4771.
52. **Thomas, A. A. M., R. J. Woortmeijer, W. Puijk, and S. J. Barteling.** 1988. Antigenic sites on foot-and-mouth disease virus type A10. J. Virol. **62**:2782–2789.
53. **Van Bekkum, J. G., H. S. Frenkel, H. H. J. Frederiks, and S. Frenkel.** 1959. Observations on the carrier state of cattle exposed to foot-and-mouth disease virus. Tijdschr. Diergeneeskd. **84**:1159–1164.
54. **Vandekerckhove, J., G. Bauw, M. Puype, J. van Domme, and M. van Montagu.** 1985. Protein-blotting on Polybrene-coated glass-fiber sheets. A basis for acid hydrolysis and gas-phase sequencing of picomole quantities of protein previously separated on sodium dodecyl sulfate/polyacrylamide gel. Eur. J. Biochem. **152**:9–19.
55. **Villanueva, N., M. Dávila, J. Ortín, and E. Domingo.** 1983. Molecular cloning of cDNA from foot-and-mouth disease virus C_1-Santa Pau (C-S8). Sequence of protein VP1 coding segment. Gene **23**:185–194.
56. **Villaverde, A., E. Martínez-Salas, and E. Domingo.** 1988. 3D gene of foot-and-mouth disease virus. Conservation by convergence of average sequences. J. Mol. Biol. **204**:771–776.
57. **Weast, R. C. (ed.).** 1982. CRC handbook of Chemistry and Physics, 62nd ed. CRC Press, Inc., Boca Raton, Fla.
58. **Weddell, G. N., D. G. Yansura, D. J. Dowbenko, M. E. Hoatlin, M. J. Grubman, D. M. Moore, and D. G. Kleid.** 1985. Sequence variation in the gene of the immunogenic capsid protein VP1 of foot-and-mouth disease virus type A. Proc. Natl. Acad. Sci. USA **82**:2618–2622.
59. **Zimmern, D., and P. Kaesberg.** 1978. 3′-Terminal nucleotide sequence of encephalomyocarditis virus RNA determined by reverse transcriptase and chain-terminating inhibitors. Proc. Natl. Acad. Sci. USA **75**:4257–4261.